



HAL
open science

Functional patterns of microbial communities of rhizospheric soils across the development stages of a young mangrove in French Guiana

Mathieu Luglia, S. Criquet, Max Sarrazin, Fabio Ziarelli, Daniel Guiral

► **To cite this version:**

Mathieu Luglia, S. Criquet, Max Sarrazin, Fabio Ziarelli, Daniel Guiral. Functional patterns of microbial communities of rhizospheric soils across the development stages of a young mangrove in French Guiana. *Microbial ecology*, 2014, 67 (2), pp.302-317. 10.1007/s00248-013-0298-9 . ird-00971793v2

HAL Id: ird-00971793

<https://ird.hal.science/ird-00971793v2>

Submitted on 4 May 2018

HAL is a multi-disciplinary open access archive for the deposit and dissemination of scientific research documents, whether they are published or not. The documents may come from teaching and research institutions in France or abroad, or from public or private research centers.

L'archive ouverte pluridisciplinaire **HAL**, est destinée au dépôt et à la diffusion de documents scientifiques de niveau recherche, publiés ou non, émanant des établissements d'enseignement et de recherche français ou étrangers, des laboratoires publics ou privés.

Functional Patterns of Microbial Communities of Rhizospheric Soils Across the Development Stages of a Young Mangrove in French Guiana

Mathieu Luglia · Stéven Criquet · Max Sarrazin ·
Fabio Ziarelli · Daniel Guiral

Abstract The functional patterns of microbial communities (microbial respiration, enzyme activities, functional diversity) and the relevant physico-chemical characteristics of rhizospheric soils were studied during the process of mudflat colonization by mangrove. The study site is a fringe mangrove stand located in Montabo Bay at Cayenne (French Guiana). It is characterized by different vegetation development stages dominated by an assemblage of *Avicennia germinans* and *Laguncularia racemosa*. Rhizospheric and surface soils were collected from three stations based on successional stages of mangrove colonization: pioneer (P), coppice (C), and young forest (F). The microbial functional patterns showed significant progressive shifts along the mangrove vegetation profile. The P stages, those most influenced by tide currents, were macroscopically characterized by hydro-sedimentary instability and micro-phytobenthic colonization of mudflat. This stage, characterized by low total organic carbon (TOC) content and quality, showed the lowest extracellular enzymatic activities and the highest functional metabolic diversities. TOC quality analyses by ^{13}C CPMAS NMR provided evidence of progressive TOC enrichment and an increasing imprint of aboveground vegetation on C quality as succession

occurs. These differences in the origin, amount, and quality of soil organic matter (SOM) of older stages exerted both a quantitative and qualitative control over microbial functional responses. This indicated the enhancement of aboveground-belowground functional linkages, leading to the expression of high decomposition activities and a functional loss and specialization of rhizospheric microbial communities.

Introduction

The Amazon River is responsible for a huge discharge of sediment into the Atlantic Ocean. A major portion of this suspended particulate matter is diverted and follows a north-western path under the influence of the North Brazil current, wind regime, and tidal currents that result in the spectacular migration of 1,600 km of subtidal mud belt along the coastline of Guianas to the Orinoco Delta [5, 15]. In French Guiana, this extension continuously leads to the formation of series of mud banks of 10–60 km in length, 20–30 km in width, and up to 5 m in thickness, which migrate at velocities ranging from 1 to more than 5 km year⁻¹ [13] along the entire coastline. They are separated by interbank areas of 15–25 km in length exposed to intensive erosion by trade-wind wave forces, generating fluid mud suspensions and delivering sediment across the intertidal zone of mud banks [5]. In contrast, in the intertidal zone, mud banks form extensive mudflats which protect the coastline from the attacks of swell and thus allow shoreline accretion. The periodic de-watering of these deposits, due to tide cycles and their colonization by diatom mats [82], progressively generates a consolidation and stabilization of the upper intertidal part of the mudflats. The arrival of propagules imported from fringing mature mangroves promotes the extension of the mangrove ecosystem benefiting from the formation of mud cracks [40] considered, in French Guiana, as responsible for 95 % of mangrove sprouting on the coastal fringe [36]. In this

M. Luglia (✉) · S. Criquet · D. Guiral
Institut Méditerranéen de Biodiversité et d'Ecologie marine et continentale (IMBE), Aix-Marseille Université, UMR CNRS IRD Avignon Université, Faculté de St-Jérôme, 13397 Marseille Cedex 20, France
e-mail: mathieu.luglia@imbe.fr

M. Sarrazin
Laboratoire des Moyens Analytiques (LAMA, US IRD 191 IMAGO), Centre IRD Guyane, Route de Montabo BP 165, 97323 Cayenne Cedex, France

F. Ziarelli
Spectropole, Fédération des Sciences Chimiques de Marseille (FR 1739 AMU/CNRS), Faculté de St-Jérôme, 13397 Marseille Cedex 20, France

environment, highly constrained by rapid and intensive hydro-sedimentary dynamics, the successional dynamic of the mangrove ecosystem gradually leads (in 50 years) to the development of series of facies, from pioneer to mature and finally to senescent [15]. With regard to the biogeographical history of mangrove extension in the world [86], these development stages present a pauci-specific feature along the 350 km of coastline of French Guiana where *Avicennia germinans* (the dominant species of the mangroves of French Guiana), *Laguncularia racemosa* (pioneer species), *Rhizophora* genus (*Rhizophora mangle* and *Rhizophora racemosa* species) [39] and very rarely *Conocarpus erectus*.

The interactions between sediment, soil organic matter (SOM) and meio- and macrofauna, responsible for changes in ground micro-topography, sediment properties, and ground water regime of these stages [15], are thought to be linked with microbial community functioning, which is a central component of biogeochemical processes and trophic dynamics that occur within the mangrove ecosystem [6, 9, 26, 33, 47, 51]. The main OM input available to the mangrove ecosystem food web comes both from the marine environment and from the decomposition processes of mangrove debris (e.g., leaves, dead wood and root exudates) mediated by microorganisms and carried out by their enzymes [22, 26, 47]. Thus, microbial functions and dynamics seem to make an essential contribution to the productivity of the mangrove ecosystem and are probably directly responsible for the well-being of mangroves [8, 17, 47]. Despite this fact, very few studies have examined the functional patterns of soil microbial communities associated with mangrove rhizosphere, especially with regard to the determinism of microbial functions involved in nutrient dynamics. The determination of enzyme activities involved in the main biogeochemical cycles (CNPS) would enable better knowledge of the role of microbial communities in mangrove ecosystems [33, 49, 59, 80].

The main goal of this study, carried out in 2010 during two hydroclimatic seasons, was thus to characterize the relationships between the development stages of mangrove, the physico-chemical characteristics of the soil, the quantity and quality of SOM, and the rhizospheric microbial functions. In addition, we have focused on soils from pioneer stages in

order to describe the prospective shifts in microbial functional patterns (a) consecutive to root assimilation and excretion of mangroves (i.e., rhizospheric vs non-rhizospheric soils) and (b) linked to species of mangroves (i.e., rhizospheric soils of *L. racemosa* vs *A. germinans*).

Materials and Methods

Study Site

The study site is a fringe mangrove stand containing an assemblage of *L. racemosa* and *A. germinans* located in an urban context (Cayenne, French Guiana, WGS 84 UTM 22 N 353 935 m E, 546 857 m N). This young mangrove, periodically inundated by semidiurnal tides (1.4 to 2.2 m tidal range), results from silt bed colonization which has begun to be deposited since 2003. Three main distinct facies are recognizable: a pioneer mangrove (i.e., P facies, height (H) < 1 m), a coppice mangrove (i.e., C facies, not cut since 2005, H < 6 m), and a young forest mangrove stand (i.e., F facies, H < 20 m), corresponding to a vegetation development profile from ocean toward inland.

Vegetation Structure of Mangrove

Three representative plots were studied for each of the three facies in order to describe the vegetation structure of the mangrove. The study plot area was defined according to stem densities: 1 m² for P facies, 25 m² for C facies, and 100 m² for F facies. Each of the dead and living individuals within the plots was tagged and counted, and the species were identified. The diameters of living trees, at a height of 10 cm (for P facies) and 130 cm (for C and F facies, and only for stems taller than 200 cm height) above the ground (DBH), were recorded. In total, 755 stems were monitored. For each facies, an estimation of the tree basal area (BA) was calculated. Dead trees and stems smaller than 2 m in height (for C and F facies) were not taken into account. The results were extrapolated for a standard area of 1 ha. From the data for density and BA for each species, an importance value index (IVI) was calculated (Eq. 1) according to Curtis and McIntosh [28]:

$$IVI_i = D_i + BA_i; \quad \text{where } i = \text{species}, \quad D_i = 100 \times \frac{n_i}{N}, \quad BA_i = 100 \times \frac{\sum_{j=1}^{n_i} BA_j}{\text{total BA}}, \quad j = \text{individual} \quad (1)$$

Soil Sampling

The soils were sampled during two hydroclimatic seasons: a wet season (WS, July, $n=25$) and a dry season (DS, November, $n=20$). The C facies was not sampled during the DS. For P

facies, three types of soil were sampled: a non-rhizospheric soil (NRZ) and two rhizospheric soils (i.e., RZA and RZL soils, respectively, for *Avicennia* and *Laguncularia*). For C and F facies, due to the strong extension of the root systems and the impossibility of specifically distinguishing the roots of

Avicennia and *Laguncularia*, only undifferentiated rhizospheric soils (RZ) were collected. For each facies and type of soil, five samples were collected. Each sample was constituted by five sub-samples randomly collected from a 100-m² plot and pooled to constitute a composite sample. Each sub-sample corresponded to 1 m² from 0–1 cm soil depth (i.e., NRZ soils of P facies, and between pneumatophores and near-surface roots of RZ soils of C and F facies) or corresponded to soil adhering to the root of uprooted seedlings of each species (i.e., RZA and RZL soils of P facies). Following sampling, all composite samples were stored at 25 °C in the darkness, except those for enzyme activity and sulphide content measurements which were stored respectively at 4 and –20 °C. Because of the fine texture and high water content of soils, the assays of almost all analyses were based on a volume of fresh soil sampled with a truncated syringe.

Physico-chemical Analysis

Water Content and Water Holding Capacity

The water content was determined after drying 100 mL of soil at 50 °C in a ventilated oven to a steady dry weight (DW). For the measurement of microbial respiration (see “Microbial Respiration (OxiTop®)”), the soil samples were standardized to the water holding capacity (WHC) according to Chamayou and Legros [23]. Briefly, the water-saturated samples were placed in polyvinyl chloride (PVC) cylinders (5 cm in diameter, 4 cm in height), which were thereafter placed on a porous ceramic plate (26.7 cm in diameter, 0.95 cm in thickness, 2.5 µm in pore size) previously saturated with distilled water during 24 h. Then, both sample PVC cylinders and ceramic plate were placed inside a closed enclosure pressurized with synthetic air (80 % N₂/20 % O₂) at 1 bar (pF 3) during 48 h. Following this treatment, the samples adjusted at the WHC were stored at 25 °C before use. The water content of these samples was determined after drying 30 g of soil at 50 °C in a ventilated oven to a steady DW.

Conductivity, pH, and Salinity

Twenty milliliters of soil was suspended in 50 mL of distilled water. After 1.5 min of agitation, conductivity was measured (inoLab® Cond Level 2 WTW). After another 1.5 min, pH H₂O was measured (inoLab® pH Level 2 WTW), and KCl was added to an approximate final concentration of 1 M. Then, after 1.5 min, pH KCl was measured.

Chloride concentration was measured by an automated colorimetric dosage (mercuric thiocyanate reactive) with a Technicon II continuous flow autoanalyzer. The salinity of in situ soil pore-water was extrapolated from the slope of the linear regression of chloride and conductivity and then adjusted to the initial soil water content.

C, N, P, and S Elemental Analyses

The dry soil was ground and sieved at 200 µm, and 20 to 50 mg DW was used for the determination of total C, N and S contents. Measurement was carried out on a CHNS elemental analyzer AS2100 ThermoQuest. Due to the almost total lack of carbonates in coastal sediments of French Guiana, total C can be attributed to the total organic C (TOC) [63]. The total P measurement was done using aqua regia and H₂O₂ digestion method according to the standard method AFNOR NF EN 13346 (X33-010). Then, phosphates released by this digestion procedure were quantified using an automated colorimetric dosage with a Technicon II continuous flow autoanalyzer.

The Olsen P measurement, which reflects the labile P pool of soil, was performed by automated colorimetric dosage with a Technicon II continuous flow autoanalyzer according to the method of Olsen et al. [68] as modified by Dabin [29]. The sulphide content (S²⁻) was measured using a potentiograph E 536 Metrohm coupled with a dosimat 665 Metrohm according to the iodometric method of Rodier et al. [77].

Solid-State ¹³C CP/MAS NMR Spectroscopy

According to the modified method of Schmidt et al. [79], the soils were pre-treated with a 10 % (v/v) hydrofluoric acid (HF) solution before analysis of the solid-state (SS) ¹³C nuclear magnetic resonance (NMR) spectroscopy in order to remove the paramagnetic compounds, concentrate the OM, and increase the signal-to-noise ratio of the resulting NMR spectra [66]. Then, 1.5 g DW of ground soil (< 200 µm) from the five samples of each facies and type of soil was pooled and the composite sample was placed in a 50-mL polypropylene falcon. Each of the composite samples (WS: n=5, DS: n=4) was suspended in approximately 40 mL of 10 % HF solution and then agitated at 50 rpm during 24 h, finally centrifuged for 10 min at 4,500 rpm, and supernatants were discarded. This HF treatment was repeated twice. In order to remove HF, the pellets were washed twice with approximately 40 mL of distilled water and centrifuged for 5 min at 6,000 rpm; then, the supernatants were discarded. The remaining pellets were suspended in approximately 10 mL of distilled water, then dried at 50 °C in a ventilated oven, and finally ground with a ceramic mortar and pestle.

The SS ¹³C NMR spectra were obtained on a Bruker Avance 400 MHz NMR spectrometer operating at a ¹³C resonance frequency of 106 MHz and using a Bruker double-bearing probe. Then, 80 mg DW of soil was placed in a zirconium dioxide rotor of 4 mm outer diameter and spun at a magic angle spinning (MAS) rate of 10 kHz. The cross-polarization (CP) technique [78] was applied with a ramped ¹H pulse starting at 100 % power and decreasing to 50 % during the contact time (i.e., 2 ms) in order to circumvent Hartmann–Hahn mismatches [25, 69]. To improve the

resolution, a dipolar decoupling GT8 pulse sequence [41] was applied during the acquisition time. To obtain a good signal-to-noise ratio in ^{13}C CPMAS experiment, 12,000 scans were accumulated using a delay of 2.5 s. The ^{13}C chemical shifts were referenced to tetramethylsilane (at 0 ppm) and calibrated with glycine carbonyl signal set at 176.5 ppm.

According to Mathers et al. [66], the SS ^{13}C CPMAS NMR spectra were divided into the four common chemical shift regions: alkyl C (0–45 ppm), *O*-alkyl C (45–112 ppm), aromatic C (112–160 ppm), and carbonyl C (160–210 ppm). Then, some chemical shift regions were further divided: *O*-alkyl C into methoxyl C (45–60 ppm), carbohydrate C (60–92 ppm) and di-*O*-alkyl C (92–112 ppm), and aromatic C into aryl C (112–142 ppm) and phenolic C (142–160 ppm). The relative intensities of each region were determined by integration using the Dmfit software version 20111221 [65]. From the data of these regions, humification (Eq. 2) and aromaticity (Eq. 3) indexes were calculated, respectively, according to Baldock and Preston [14] and Hatcher et al. [45].

$$\text{Humification index} = \frac{\text{Alkyl C}}{\text{O-alkyl C}} \quad (2)$$

$$\text{Aromaticity index} = \frac{\text{Aromatic C}}{(\text{Alkyl C} + \text{O-alkyl C} + \text{Aromatic C})} \times 100 \quad (3)$$

Finally, according to Mathers et al. [66], to obtain C-quantified data instead of only C proportions, the spectral percentages of each NMR region were multiplied by both the TOC value of sample residue and enrichment factor (i.e., sample residue mass/sample raw mass). The TOC contents of acid-soluble fractions were deduced from these results.

The signals in alkyl C region are characteristic of methylenic structures of lipids, waxes, cutins, suberins, resins of plants, and other aliphatic biomacromolecules [3, 31, 76] and likewise of amino acid C [52]. The signals in *O*-alkyl C region are characteristic of many molecules, the main ones in soils being recognized to be polysaccharides, celluloses, hemicelluloses, and alcohols [52, 74], some of which could be present in our acid-soluble fraction. The signals in the aromatic C region are characteristic of recalcitrant C to degradation found in lignin (protonated C, C-substituted aromatic C, and phenolic C) and tannins, although the aromatic amino acids of proteins and the phenolic acids of cutins also occur in this region [52, 74]. Finally, the signals in carbonyl C region are characteristic of carboxyl C, amides, and esters [52, 74].

Microbial Respiration (OxiTop®)

Microbial respiration (MR) was measured with an OxiTop® automatic system WTW to monitor O_2 consumption according to Alarcón-Gutiérrez et al. [2]. The monitoring of the pressure in the closed enclosure containing the soil allows

the calculation of the consumed O_2 amount by MR. Twenty grams of soil at the WHC was placed in a jar (600 mL) with a rubber vessel containing four pellets of NaOH to trap the CO_2 and sealed with an OxiTop® head. The jar was incubated in a thermostatic cabinet Liebherr at 30 °C in darkness to prevent photosynthetic activity, and O_2 depression was recorded every 8 min during 2 days. At the end of the experiment, data were downloaded from OxiTop® head with an OxiTop® IR controller OC 110 WTW. The MR was calculated from the slope of the depression curve and expressed in milligram O_2 consumed per day and per kilogram of soil DW ($\text{mg O}_2 \text{ day}^{-1} \text{ kg}^{-1} \text{ DW}$).

Enzyme Activities

The enzyme activities assayed were β -glucosidases (β -glu), ureases (Ure), acid phosphomonoesterases (AcP), arylsulphatases (AryS), fluorescein diacetate hydrolases (FDA), and lipases (Lip) [37]. The enzyme assays were performed in three replicates and one control (substrate added after incubation) for each sample. A unit (U) of enzyme activity was defined as micromole of hydrolyzed substrate per minute and per gram of soil DW ($\text{U g}^{-1} \text{ DW}$).

The β -glu activity was assessed by measuring the *p*-nitrophenyl β -D-glucopyranoside (*p*-NPG) hydrolysis to *p*-nitrophenol (*p*-NP) according to Eivazi and Tabatabai [34]. Two milliliters of sediment sample was suspended in 4 mL of modified universal buffer (MUB) [83], pH 6.0, and 1 mL of 5 mM *p*-NPG solution and thereafter incubated for 1 h at 37 °C. The reaction was stopped by adding 1 mL of 0.5 M CaCl_2 solution and 4 mL of 0.1 M tris-hydroxymethyl-aminomethane (THAM) solution, pH 12, and the solution was finally centrifuged for 10 min at 4,000 rpm.

AcP activity was assessed by measuring the *p*-nitrophenyl phosphate (*p*-NPP) hydrolysis to *p*-NP according to Tabatabai and Bremner [84]. Two milliliters of sediment sample was suspended in 4 mL of MUB, pH 6.5, and 1 mL of 5 mM *p*-NPP solution and thereafter incubated for 30 min at 37 °C. The reaction was stopped by adding 1 mL of 0.5 M CaCl_2 solution and 4 mL of 0.5 M NaOH solution, and the solution was finally centrifuged for 10 min at 4,000 rpm.

AryS activity was assessed by measuring the *p*-nitrophenyl sulphate (*p*-NPS) hydrolysis to *p*-NP according to Tabatabai and Bremner [85]. Two milliliters of sediment sample was suspended in 4 mL of 0.5 M sodium acetate buffer, pH 5.8, and 1 mL of 5 mM *p*-NPS solution and thereafter incubated for 1 h at 37 °C. The reaction was stopped by adding 1 mL of 0.5 M CaCl_2 solution and 4 mL of 0.5 M NaOH solution, and the solution was finally centrifuged for 10 min at 4,000 rpm.

For these three enzyme activities, the amount of released *p*-NP was measured in the supernatant at 412 nm with a spectrophotometer Specord® 205 Analytik Jena.

Ure activity was assessed by measuring the urea ($\text{CO}(\text{NH}_2)_2$) hydrolysis to NH_4^+ according to Kandeler and Gerber [50]. Two milliliters of sediment sample was incubated for 4 h at 37 °C with 0.5 mL of 4.8 g L^{-1} urea solution. The reaction was stopped by adding 10 mL of 1 M acidified KCl solution, then agitated for 30 min at 230 rpm to extract NH_4^+ ions, and the solution was finally centrifuged for 20 min at 4,000 rpm. The dosage of NH_4^+ , according to the method of Koroleff [54] as modified by Grasshoff and Johansen [42], was done on 2.5 mL of supernatant with 1 mL of phenol-prussiate reactant and 1 mL of alkaline dichloroisocyanurate reactant. At 6 h later in darkness, the absorbance was measured at 660 nm with a spectrophotometer Specord® 205 Analytik Jena.

FDA activity was assessed by fluorescence in microplate by measuring the fluorescein diacetate hydrolysis to fluorescein according to the modified method of Green et al. [43]. The buffer pH used was 7.0 instead of 7.6 to avoid potential non-enzymatic interferences as recommended by Alarcón-Gutiérrez et al. [4]. Two milliliters of sediment sample was suspended in 9 mL of 0.1 M phosphate buffer, pH 7.0. Then, 180 μL of this suspension was incubated for 3 h at 30 °C with 20 μL of 20 mM fluorescein diacetate solution (in acetone).

Lip activity was assessed by fluorescence in microplate by measuring the fluorescein dilaurate (FDL) hydrolysis to fluorescein according to the modified method of Gupta et al. [44]. Two milliliters of sediment sample was suspended in 8 mL of 0.1 M phosphate buffer, pH 7.0, with 1 % of Triton X-100. Then, 180 μL of this suspension was incubated for 3 h at 30 °C with 20 μL of 20 mM FDL solution (in isopropanol).

For these two enzyme activities, the amount of released fluorescein was measured every 5 min at an excitation wave of 490 nm and an emission wave of 514 nm with a microplate reader Infinite® M200 Tecan. The results were expressed on the basis of optimum hydrolysis rate detected during the incubation.

Community Level Physiological Profile (CLPP, Biolog EcoPlates™) Assessment

The Biolog EcoPlates™ were used to determine the community level physiological profiles (CLPPs) of mangrove soils and thus to assess the potential metabolic diversity of microbial communities. A fresh mass equivalent to 1 g DW of soil was suspended in 10 mL of 0.1 % (*v/v*) sterile sodium pyrophosphate solution and then agitated for 30 min at 230 rpm to extract the soil microbial community. Thereafter, the suspension was 100-fold (*v/v*) diluted with a 0.85 % (*v/v*) sterile NaCl solution, and 125 μL of this suspension was inoculated in each well. The microplate was immediately agitated for 5 min at 1,300 rpm with a vibrating microplate

shaker Titramax 1000 Heidolph®, and time 0 optical densities (ODs) of wells were measured at 590 nm with a microplate reader Infinite® M200 Tecan. Finally, the microplate was incubated at 26 °C during 5 days in darkness, and well OD measurements were done two or three times a day. For each measuring time and microplate replicate, the average well color development (AWCD) was calculated and then the growth curve was plotted. The time to reach an AWCD of 0.5 (AWCD_{0.5}) was determined by extrapolation for each microplate replicate. From this time, the total number of metabolized substrates (metabolic richness, *S*) was determined using an OD of 0.1 as threshold for positive response, and the Shannon's diversity (*H'*) and Pielou's evenness (*J'*) indexes were calculated. Finally, at the time of AWCD_{0.5}, OD values of each well were used subsequently in the principal component analysis (PCA) of soil CLPPs.

Statistical Analysis

Means and standard deviations were determined for each set of replicates (*n*=5). Analyses of variance (ANOVA) were used to test the effect of soil factor (one-way ANOVA) on a quantitative variable, at a significance level of $P < 0.05$ (*n*=5). Thereafter, we used the post hoc test of multiple comparisons of Tukey (honestly significant difference, HSD) in order to verify whether the various modalities of the tested factor were significantly different from each other, at a significance level of $P < 0.05$.

Pearson's correlation coefficients (*r*) were used to assess the degree of linear relationship between two quantitative variables, at a significance level of $P < 0.05$ (WS: *n*=25, DS: *n*=20; except for NMR composite data where *n* was 5 and 4, respectively).

PCA were used to compare the soils of various facies of the mangrove on physico-chemical properties (*n*=45), TOC contents (*n*=9), and microbial functional characteristics (*n*=45). Following the variables, we used for the similarity matrix calculation Pearson's correlation coefficient or the covariance. Thereafter, multivariate analyses of variance by permutation (PERMANOVA) [71] were used to test the effect of soil or rhizospheric factor (one-way PERMANOVA) on a set of quantitative variables, at a significance level of $P < 0.05$, with 5,000 permutations. Then, the test of pairwise multiple comparisons by permutation was used in order to verify that parameters of various modalities of the tested factor were significantly different, at a significance level of $P^* < (0.05/i)$ with 5,000 permutations, where *i* was the total number of comparisons.

All of these analyses were performed using XLSTAT software version 2009.3.02 (Addinsoft™, France), except for one-way PERMANOVA and pairwise multiple comparisons by permutation analyses, which were performed using

PMANOVA free computer program (<http://pages.usherbrooke.ca/jshipley/recherche/my%20programs.htm>).

Results

Vegetation Structure of Mangrove

The P facies was characterized by very high seedling density (10^6 stems ha^{-1}) dominated by *L. racemosa* (65 %) (Table 1). Moreover, seedling spatial distribution was heterogeneous, resulting in a patchy vegetal cover, separated by non-vegetated zones colonized by micro-phytobenthos. A marked decrease in tree density occurs from P to F facies according to a self-thinning process. Comparatively to the P facies, we observed a survival rate of 1/25 individuals within the C facies and 1/150 individuals within the F facies, with the progression of the percentage of dead standing trees from 0 to 30 (Table 1). These high mortality rates during the stem exclusion stages affect differently the two species. Relative to P facies and *A. germinans*, we observed a survival rate of 1/15 individuals within the C facies and 1/65 individuals within the F facies. In the case of *L. racemosa*, we observed the survival of 1/35 individuals within the C facies and 1/530 individuals within the F facies (Table 1).

The BAs, although not directly comparable between the P facies and the other two (i.e., diameter measured at 10 cm in height for P facies instead of 130 cm), were higher ($21 \text{ m}^2 \text{ ha}^{-1}$) for P facies. They showed a strong variability and seemed to stabilize to $17 \text{ m}^2 \text{ ha}^{-1}$ for C and F facies (Table 1). The IVIs of *Avicennia* and *Laguncularia* for P and C facies were about 100 but became 162 for *Avicennia* against 38 for *Laguncularia* for F facies (Table 1), reflecting the strong competitive value of *Avicennia*, which grows faster and higher, while *Laguncularia*, overtopped and shaded, gradually dies.

Table 1 Vegetation structure of mangrove stand

		Facies			
		P	C	F	
Ind. nb/ha		$1.175 \times 10^6 \pm 0.757$	$5.84 \times 10^4 \pm 0.396$	$11.4 \times 10^3 \pm 0.566$	
Living trees (%)	Avi.	35±10	56±7	81±8	
	Lag.	65±10	44±7	18±8	
	Rhi.	0	0	2±1	
Dead standing trees (%)		0	12±8	30±7	
BA	Total	(m^2/ha)	21±13	17±3	17±5
	Avi.	(%)	59±16	50±5	82±8
	Lag.	(%)	41±16	51±5	18±8
	IVI	Avi.	102	105	162
	Lag.	98	95	38	

Values are means ($n=3$) \pm standard deviations
P pioneer facies, *C* coppice facies, *F* young forest facies, *Avi* *Avicennia*, *Lag* *Laguncularia*, *Rhi* *Rhizophora*, *BA* tree basal area, *IVI* importance value index

Physico-chemical Properties of Soils

During the WS, several parameters (i.e., TOC, total N and S, S^{2-} , Olsen P, $\text{H}_2\text{O}_{\text{WHC}}$) showed similar patterns of change across the facies of the mangrove (Table 2). For this set of variables, it appeared that the older the vegetation stages, the higher the variable values. In contrast, salinity showed a quite different pattern. For this parameter, the highest values were observed in the pioneer stand, while the C and F facies showed the lowest values. During the DS, similar patterns in the variable distribution were observed according to the facies gradient. However, salinity and Olsen P showed constant values.

PCA and PERMANOVA showed that the differences of physico-chemical characteristics between the soils for both seasons were highly significant (WS: $\chi^2=95.7$, DS: $\chi^2=72.3$, both $P < 0.001$). Nevertheless, there was no significant difference in the physico-chemical characteristics between RZA and RZL soils of P facies for the two seasons (WS: $\chi^2=7.9$, $P^*=0.795$; DS: $\chi^2=15.7$, $P^*=0.203$). This was also true for NRZ soils relative to RZA and RZL soils of P facies (WS: $\chi^2=27.7$, 29.7 , $P^* > 0.005$; DS: $\chi^2=24.5$, 24.7 , $P^* > 0.008$). During the WS, soils of older stages (i.e., C and F facies) were clearly discriminated relative to those of P facies (C facies: $\chi^2=50.8$, 55.6 , 56.7 , $P^* < 0.0001$; F facies: $\chi^2=55.5$, 71.0 , 82.7 , $P^* < 0.0001$) on the PC1 due to their higher values of TOC and $\text{S}^{2-}/\text{totS}$ and OlsP/totP ratios. Moreover, soils of C and F facies were segregated ($\chi^2=38.0$, $P^* < 0.001$) on PC2, mainly by pH_{KCl} . During the DS, soils of F facies were still discriminated relative to those of P facies ($\chi^2=44.8$, 61.5 , 63.2 , $P^* < 0.0002$) on the PC1 but, unlike the WS, this was mainly due to higher TOC content values.

Soil TOC Content and Quality

Following HF treatment, we observed a strong mass loss in soils, ranging from 70 to 80 % (Table 3). This was mainly due

Table 2. Physico-chemical properties of mangrove soils

Characteristics	WS						DS										
	P			C			F			P			F				
	NRZ	RZA	RZL	RZ	RZ	RZ	RZ	RZ	NRZ	RZA	RZL	NRZ	RZA	RZL	NRZ	RZA	RZL
Water content at WHC (g kg ⁻¹)	381±0 b	383±4 b	382±4 b	412±4 a	410±4 a	410±4 a	390±6 b	388±3 b	391±6 b	402±5 a							
Salinity	61±21 a	39±5 b	41±8 ab	4±2 c	17±9 c	17±9 c	41±7 a	36±1 a	37±1 a	40±2 a							
pH _{KCl}	7.3±0.1 a	6.9±0.2 b	6.9±0.2 b	6.8±0.1 b	7.5±0.2 a	7.5±0.2 a	7.4±0.0 a	7.0±0.2 b	6.8±0.1 b	6.8±0.1 b							
TOC (g kg ⁻¹ DW)	14.7±3.5 b	13.5±1.5 b	12.9±1.7 b	19.9±1.0 a	22.8±1.6 a	22.8±1.6 a	13.7±1.7 b	12.3±1.4 b	13.3±2.4 b	19.0±1.5 a							
Total N (g kg ⁻¹ DW)	1.4±0.2 c	1.5±0.1 c	1.4±0.1 c	2.0±0.1 b	2.2±0.1 a	2.2±0.1 a	1.5±0.1 b	1.5±0.2 b	1.6±0.1 b	2.0±0.1 a							
Molar C/N ratio	11.9±1.4 ab	10.4±0.7 b	10.4±0.8 b	11.9±0.5 ab	12.0±0.4 a	12.0±0.4 a	10.4±1.0 ab	9.4±0.8 b	9.6±1.1 ab	11.1±0.3 a							
Total S (mg kg ⁻¹ DW)	2,050±520 b	1,200±122 b	1,260±270 b	3,200±316 a	4,060±764 a	4,060±764 a	1,300±82 b	1,280±409 b	1,240±279 b	2,940±410 a							
S-S ²⁻ (mg kg ⁻¹ DW)	2±2 b	9±8 b	5±3 b	1,287±274 a	1,675±559 a	1,675±559 a	3±2 b	8±12 b	7±9 b	128±70 a							
Total P (mg kg ⁻¹ DW)	463±130 a	507±54 a	496±53 a	541±63 a	584±54 a	584±54 a	590±27 a	572±26 a	581±24 a	584±22 a							
Olsen P (mg kg ⁻¹ DW)	60±6 b	61±14 b	54±9 b	86±12 b	159±47 a	159±47 a	67±4 a	59±11 ab	51±8 b	65±3 a							

Values are means (n=5) ± standard deviations. For each season, values followed by the same letters in a row do not differ significantly from each other at P<0.05.

WS wet season, DS dry season, P pioneer facies, C coppice facies, F young forest facies, NRZ non-rhizospheric soil, RZ rhizospheric soil, A Avicennia, L Laguncularia

Microbial Respiration

MR had similar patterns across the mangrove facies for both seasons (Fig. 2). Higher levels of MR were observed in RZ soils of C and F facies for both seasons, showing values three- to eightfold higher than those of P facies. There was no significant difference of MR between RZA and RZL soils of P facies for the two seasons (Fig. 2). However, the MR of NRZ soils during the DS was significantly twofold higher than those of the two other soils of P facies. Finally, we

to the mineralogical composition of these Amazonian sediments, rich in HF-soluble aluminum silicates and iron oxyhydroxides. The molar C/N ratios of residues were higher than those of soils before HF treatment, showing a preferential loss of organic compounds with relatively high N content (Table 3). The percentages of TOC in acid-soluble fraction were high overall and higher for NRZ soils than for the others. These proportions decreased along the facies gradient for both seasons, reflecting a lower acid-soluble OM (ASOM) for the older soils (Table 3).

For all facies and for both seasons, the alkyl C and O-alkyl C regions dominated over the aromatic C and carbonyl C regions of acid-insoluble fraction (i.e., residue) of SOM (Table 4). Within the O-alkyl C region, the carbohydrate C region broadly dominated over the other two and also over the aromatic C and carbonyl C regions. The contribution of alkyl C to TOC for both seasons increased according to the facies gradient from approximately 20 to 30 % (Table 4). That of O-alkyl C was about 30 % across the facies for both seasons, with RZL soils of P facies exhibiting the highest percentages (i.e., 33 and 35 %, respectively, in WS and DS). For the two seasons, the proportions of aromatic C and carbonyl C showed little variation across the facies. The increase of TOC content in soils observed through the developmental stages of mangrove mainly resulted in the increase of OC as alkyl C and O-alkyl C (Table 4). The humification index slightly increased according to the facies gradient for both seasons (ranging from 0.6 to 1) (Table 4). By contrast, RZ soils of F facies showed the lowest values of aromaticity index for both seasons (i.e., 19 and 17 %, respectively, in WS and DS). Results of PCA (Fig. 1b) evidenced a contrast between the soils of P facies and those of older stages on PC1 for both seasons. Thereby the soils of C and F facies were discriminated in the positive area of PC1 due to their higher values in OC like alkyl C and carbohydrate C. The main variable expressed on PC2 was acid-soluble C (on the positive side), accounting for 79.6 % of the variance explained by this axis. We observed that the soils were closer to each other in DS than in WS on PC2. Thus, PC2 depicted seasonal variations of acid-soluble C content in soils, with higher variations during the WS than the DS.

Table 3 Characterization of mangrove soils after HF treatment

Season	Facies	Soil	Residue	Acid-soluble fraction			
				Mass loss % of raw soil	C/N ratio Molar	C % of TOC	N % of total N
WS	P	NRZ	74.3	12.3	30.3	31.5	11.6
		RZA	79	12.3	21.5	33.5	6.7
		RZL	78.2	11.4	27.2	33.3	8.5
	F	CZ	78.6	12.2	26	27.9	11.1
		RZ	77.7	13.8	18.6	29.6	7.5
		NRZ	78	11.5	26.2	32.9	8.3
DS	P	RZA	78	11.2	24.9	37.7	6.2
		RZL	73.8	11.8	20	34.6	5.5
		RZ	75.7	12.6	19.1	28.9	7.3

Values are based on a composite sample

WS wet season, DS dry season, P pioneer facies, C coppice facies, F young forest facies, NRZ non-rhizospheric soil, RZ rhizospheric soil, A *Avicennia*, L *Laguncularia*

observed significant and strong positive correlations between MRs and TOC contents for both seasons (WS: $r=0.921$, DS: $r=0.860$, both $P<0.001$).

Enzyme Activities

β -Glu, Ure, AcP, and Lip activities varied similarly across the facies with increasing activities from P to F facies for the two seasons (Fig. 3). Among these, β -glu and Lip were the two enzymes which showed the strongest activity increases between the facies (respectively five- and 20–50-fold higher between P and F facies). They showed significant and strong positive correlations for both seasons, respectively, with TOC content (WS: $r=0.919$, DS: $r=0.901$, both $P<0.001$) and OC content as alkyl C (WS: $r=0.962$, $P<0.01$; DS: $r=0.985$, $P<0.05$). The FDA showed constant levels of activity across the facies for the two seasons, except for RZ soils of F facies which showed two- to threefold higher activity during the DS. A significant effect of season was observed on Ure and ArylS activities of various facies. Their activity levels through the facies were overall higher in the WS than in the DS (Fig. 3). Finally, within the P facies, results showed that globally there was no significant difference between the three soils (Fig. 3).

CLPPs and PCA of Microbial Functions

Similar patterns of S were observed along the mangrove facies for the two seasons with a higher S during the DS (Fig. 4). RZA and RZL soils of P facies showed the highest S s for both seasons. The J 's (data not shown) showed high values ($0.92<J<0.94$), which did not differ significantly from each other between the facies for the two seasons.

As for S , similar trends for H' were observed across the facies for the two seasons, with higher diversity during the DS (Fig. 4). The H' decrease observed throughout the development stages of mangrove was only related to the S decrease

and not to the efficiency decrease of substrate utilization (i.e., OD of a given positive well). There were no differences of H' between the three soils of P facies for the two seasons. The lowest H' s were observed in RZ soils of C and F facies for both seasons. Moreover, RZ soils of F facies showed the strongest fine-scale spatial heterogeneity of H' . Results of PCA, performed on the different Biolog C substrates (Fig. 5), revealed that differences of catabolic profiles of soils between P, C, and F facies in the WS and between P and F facies in the DS were highly significant (WS: $\chi^2=187.4$, DS: $\chi^2=158.9$, both $P<0.001$). Nevertheless, results showed that there was no significant difference of catabolic profiles between RZA and RZL soils of P facies for the two seasons (WS: $\chi^2=34.2$, $P^*=0.984$; DS: $\chi^2=60.3$, $P^*=0.260$). A contrast between soils of P facies and those of older stages was observed on PC1 for the two seasons. The soils of C and F facies were discriminated in the negative area of PC1 due to their higher utilization of D1, C1, and H4 (i.e., methylenic structures) and their lower utilization of E1 and F1 (i.e., polysaccharide polymers). Another contrast between soils of P and F facies was observed on PC2 which was characteristic of season effect. During the WS, the soils of F facies were found in the positive area of PC2 due to their higher utilization of D-galacturonic acid (B3) and inversely in the DS.

Finally, a PCA (Fig. 1c) was performed on all the microbial functions (i.e., MR, enzyme activities and CLPPs) to investigate which best discriminate the different facies. Multivariate analysis confirmed the previous results in that, for both seasons, P soils were clearly discriminated from those of C and F facies due to higher enzymatic activities (i.e., β -glu, AcP, and Lip) and respiration rates as well as lower functional diversity (WS: $\chi^2=117.2$, DS: $\chi^2=134.9$, both $P<0.001$). By contrast, there was no significant multivariate difference of functional patterns between RZA and RZL soils of P facies for both seasons (WS: $\chi^2=9.1$, $P^*=0.911$; DS: $\chi^2=32.0$, $P^*=0.010$).

Table 4 TOC content, humification, and aromaticity indexes derived from SS ¹³C CP-MAS NMR spectra of mangrove soils

Season	Facies	Soil	Residue		Chemical shift regions of spectrum (ppm)												Humification index		Aromaticity index			
			Acid-soluble fraction	Residue	O-alkyl C				Aromatic C				Alkyl C/O-alkyl C				Ratio	%	Ratio	%		
					Alkyl C		Methoxyl C		Carbohydrate C		Di-O-alkyl C		Aryl C		Phenolic C		Carbonyl C					
					0-45	45-60	60-92	92-112	112-142	142-160	160-210	Alkyl C/O-alkyl C										
					TOC content (g kg ⁻¹ DW)																	
WS	P	NRZ	4.5	(30.3)	2.7	(18.6)	1.1	(7.2)	2.9	(19.8)	0.7	(5.0)	1.3	(8.7)	0.6	(4.3)	0.9	(6.1)	0.6			20.5
			2.9	(21.5)	3.8	(28.4)	0.8	(6.2)	2.4	(17.9)	0.5	(3.9)	1.6	(11.7)	0.4	(3.2)	1.0	(7.3)	1.0			20.8
			3.5	(27.2)	2.7	(21)	0.7	(5.5)	2.8	(22.0)	0.7	(5.1)	1.4	(10.6)	0.5	(4.1)	0.6	(4.6)	0.6			21.5
C	RZ	RZ	5.2	(39)	4.8	(24.2)	1.3	(6.4)	3.2	(16.1)	0.8	(4.2)	1.6	(8.2)	1.5	(7.6)	1.5	(7.3)	0.9			23.6
			4.2	(18.6)	6.9	(30.4)	1.3	(5.6)	4.8	(21.0)	1.0	(4.2)	2.7	(11.7)	0.6	(2.7)	1.3	(5.8)	1.0			19
			3.6	(26.2)	3.4	(25.1)	0.7	(5.5)	2.7	(20.1)	0.5	(3.9)	1.4	(10.2)	0.5	(3.4)	0.8	(5.6)	0.9			19.9
DS	P	RZA	3.1	(24.9)	2.8	(22.7)	0.7	(6.0)	2.6	(21.2)	0.7	(5.5)	1.2	(9.4)	0.5	(3.7)	0.8	(6.6)	0.7			19.2
			2.7	(20.0)	3.0	(22.5)	1.1	(8.5)	2.8	(20.9)	0.8	(5.6)	1.6	(11.9)	0.6	(4.1)	0.9	(6.4)	0.6			21.7
			3.6	(19.1)	6.1	(31.9)	0.9	(4.7)	3.8	(19.9)	0.9	(4.7)	1.8	(9.6)	0.6	(2.9)	1.4	(7.2)	1.1			17

Values are based on a composite sample. Values in brackets are OC expressed in % of TOC

WS wet season, DS dry season, P pioneer facies, C coppice facies, F young forest facies, NRZ non-rhizospheric soil, RZ rhizospheric soil, A Avicennia, L Laguncularia

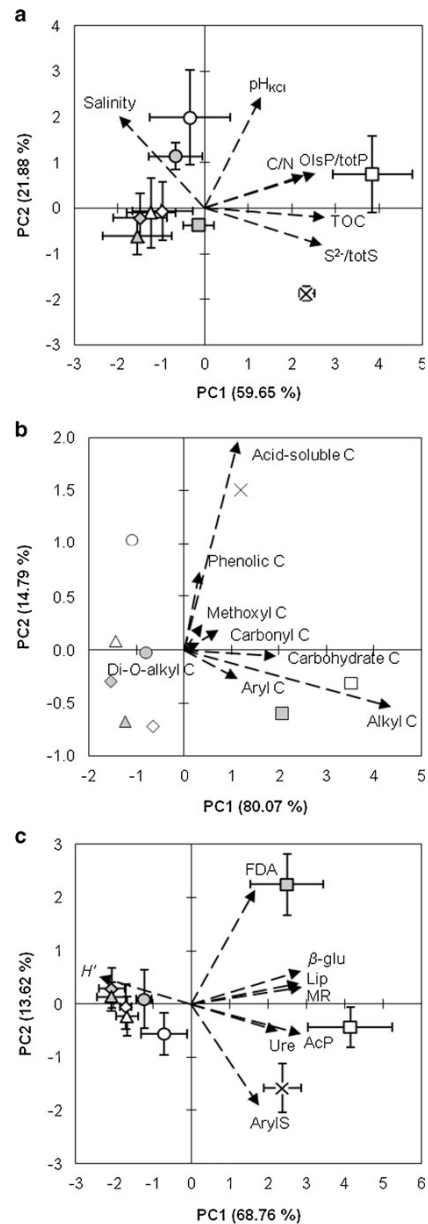


Fig. 1 PCA of environmental and microbial characteristics of mangrove soils. **a** Biplot of PCA (Pearson) of physico-chemical properties accounting for 81.53 % of total variance. **b** Biplot of PCA (covariance) of TOC contents derived from SS ¹³C NMR spectroscopy accounting for 94.86 % of total variance. **c** Biplot of PCA (Pearson) of microbial respiration, enzyme activities, and functional diversity accounting for 82.39 % of total variance; vector scale, ×3. Symbols depict means ($n=5$) with standard deviations (in brackets) on PC1 and PC2, except for **b** (composite samples). White symbols, wet season; grey symbols, dry season; circle, non-rhizospheric soil of pioneer facies; diamond, rhizospheric soil of *Avicennia* of pioneer facies; triangle, rhizospheric soil of *Laguncularia* of pioneer facies; cross, rhizospheric soil of coppice facies; square, rhizospheric soil of young forest facies

Discussion

Mangrove and Soil Characteristics

Establishment of the mangrove began by the concomitant colonization of sediments by both *Avicennia* and *Laguncularia* seedlings. Following this first step, competition phenomena (availability of nutrients and light) occurred between these species. Since *Avicennia* is known as being a taller species than *Laguncularia*, it was logical that *Laguncularia* was progressively overtopped and finally excluded by *Avicennia* as succession proceeded. The scenario observed was coherent with those described by Peltier [70], Betoulle [18], and Cadamuro [21] in other sites of French Guiana. It is representative of an ocean front mangrove which shows a generic and rapid successional dynamic, benefiting from nutrient enrichment from the Amazon and favorable climatic conditions due to its situation close to the equator. The succession we observed resulted in a young forest which was not an ultimate successional stage in mangrove ecosystems but which allowed the development of more matured soils with enhanced aboveground–belowground linkages.

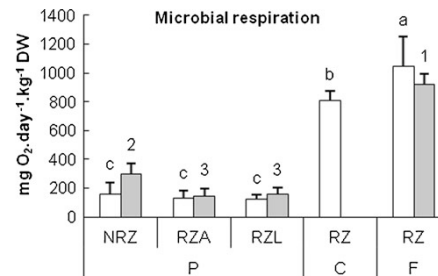


Fig. 2 Microbial respiration of mangrove soils. Bars depict means ($n=5$) with standard deviations (in brackets). For each season, bars followed by the same letters or numbers do not differ significantly from each other at $P < 0.05$. White bars, wet season; grey bars, dry season; P, pioneer facies; C, coppice facies; F, young forest facies; NRZ, non-rhizospheric soil; RZ, rhizospheric soil; A, *Avicennia*; L, *Laguncularia*

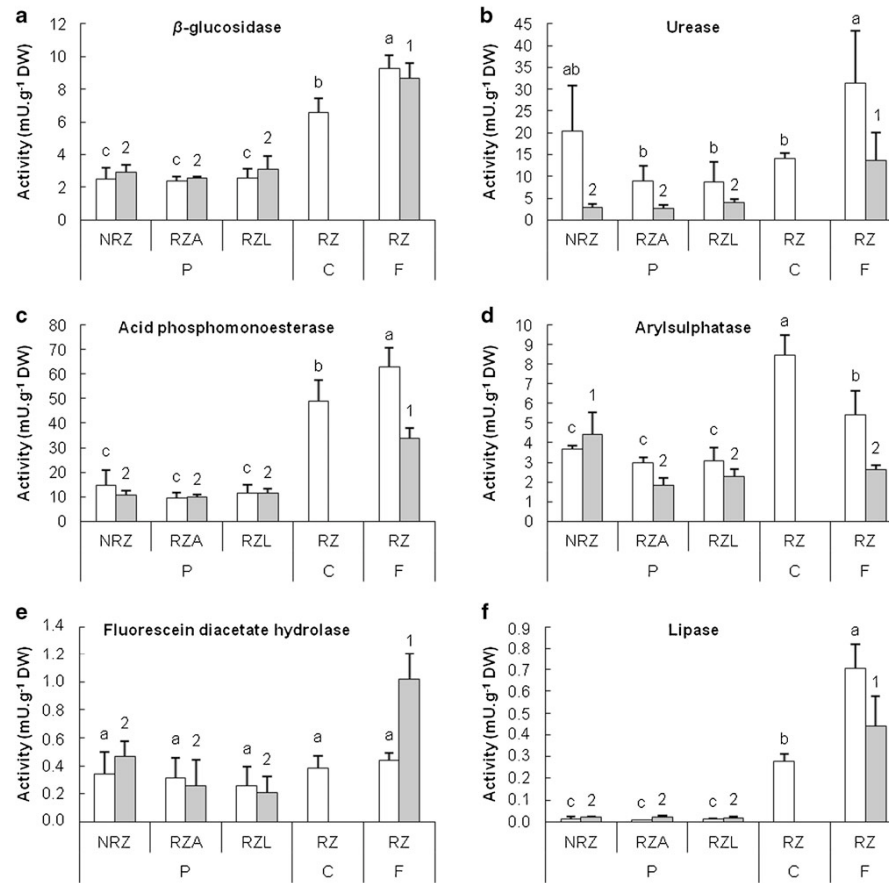


Fig. 3 a–f Enzyme activities of mangrove soils. Bars depict means ($n = 5$) with standard deviations (in brackets). For each season, bars within a graph followed by the same letters or numbers do not differ significantly from each other at $P < 0.05$. White bars, wet season; grey bars, dry

season; P, pioneer facies; C, coppice facies; F, young forest facies; NRZ, non-rhizospheric soil; RZ, rhizospheric soil; A, *Avicennia*; L, *Laguncularia*

The soils of the different facies had similar textural properties (e.g., mineralogy, particle size distribution, macro- and micro-porosity) (data not shown). In contrast, other physico-chemical characteristics showed significant spatial and seasonal variations. Results, especially those of the WS, highlighted that ocean distance and micro-topography, allowing rainwater stagnation, were prevailing factors with regard to spatial variations of soil salinities. This freshwater stagnancy led to occasional reducing conditions highlighted by increases in sulphide content (up to 50% of total S) and of

the bio-available fraction of P (i.e., Olsen P), probably released from the iron-bound P pool ($\text{Fe}(\text{OOH})\approx\text{P}$) under reduced conditions [35].

Results for TOC content (< 2%) in mangrove soils were consistent with those of many studies on mangrove ecosystems [57]. The values of C/N ratios observed were around 11, while the majority of the world intertidal mangrove sediments exceeded C/N ratios of 20 [57]. These low C/N ratios indicated that the SOM was probably not mainly derived from mangrove debris but much more from marine imported OM

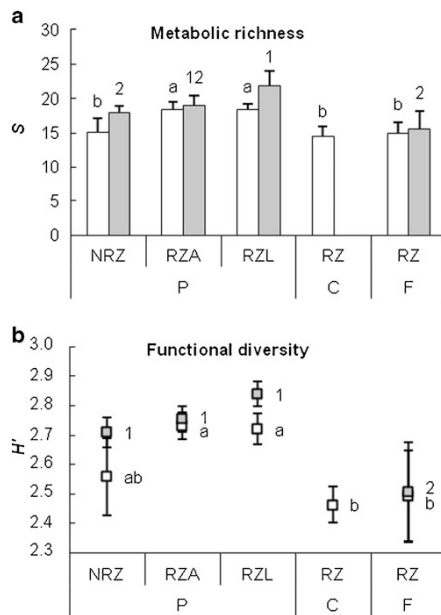


Fig. 4 a Metabolic richness (S) and b functional diversity (H') derived from Biolog EcoPlates™ analyses of mangrove soils. Markers and bars depict means ($n=5$) with standard deviations (in brackets). For each season, means within a graph followed by the same letters or numbers do not differ significantly from each other at $P < 0.05$. White markers and bars, wet season; grey markers and bars, dry season; P, pioneer facies; C, coppice facies; F, young forest facies; NRZ, non-rhizospheric soil; RZ, rhizospheric soil; A, *Avicennia*; L: *Laguncularia*

[64]. This reflected both the youth of the mangrove stand and the exportation of the majority of mangrove inputs (e.g., litter) by the tides.

Nevertheless, results from SS ^{13}C NMR analysis indicated a shift of soil TOC quality across the mangrove development profile: the more mature the facies, the richer the soil in the different C pools, especially alkyl C and carbohydrate C (both accounting for about 60 % of TOC). During HF treatment, a large fraction of TOC (20–30 %) was lost as acid-soluble C. According to Skjemstad et al. [81], HF does not involve significant changes in the distribution of chemical functions of OM. However, according to Schmidt et al. [79], Hatcher et al. [46], and Preston et al. [73], a small and preferential loss of labile carbohydrates may occur. Thus, from these observations, we conclude that both the enrichment and quality of TOC observed must reflect an increased imprint of mangrove vegetation on SOM. Similar differences in organic sources, contents, and qualities have also been observed in other

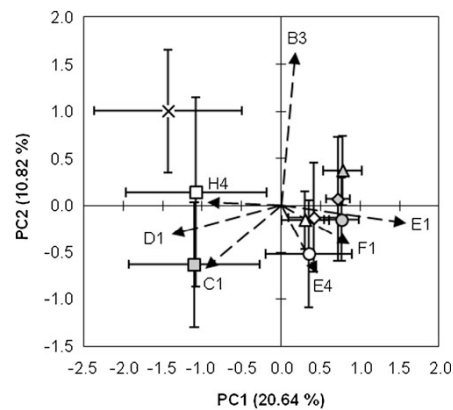


Fig. 5 PCA (covariance) of potential catabolic profiles of mangrove soils; biplot of PCA on 27 substrates accounting for 31.46 % of total variance; vector scale: $\times 3$; only the most driving variables are represented. B3, D-galacturonic acid; C1, tween 40; D1, tween 80; E1, α -cyclodextrin; E4, L-threonine; F1, glycogen; H4, putrescine. Symbols depict means ($n=5$) with standard deviations (in brackets) on PC1 and PC2. White symbols, wet season; grey symbols, dry season; circle, non-rhizospheric soil of pioneer facies; diamond, rhizospheric soil of *Avicennia* of pioneer facies; triangle, rhizospheric soil of *Laguncularia* of pioneer facies; cross, rhizospheric soil of coppice facies; square, rhizospheric soil of young forest facies

mangrove forests [11, 20, 72], the high intertidal forests being an important deposition area of refractory mangrove detritus, while the low intertidal forests, exposed to strong currents, prevent such deposits [58].

Another original result concerned the quality of SOM of NRZ soils from P facies. These were characterized by higher % of ASOM than the RZ soils of the two mangrove species. The explanation for this enrichment may be provided by the initial colonization of mudflat surface by marine organisms. In French Guiana, before the rooting of seedlings, the mudflats are colonized at low tide mainly by micro-phytobenthic diatoms. These microalgae are known to produce large quantities of extracellular polymeric substances (EPS) resulting in the formation of biofilm at the water–sediment interface. Thus, as also suggested by Debenay et al. [30], such substances may explain the ASOM enrichment observed in the NRZ plots, mangrove seedlings, and their root exudates being of lesser importance for soil TOC quality.

Microbial Metabolism vs Environmental Factors

Microbial Respiration

The mangrove formations develop particular root systems resulting in a dense network of near-surface roots in which

the aerenchyma tissues are connected with lenticels on pneumatophores, prop roots, and buttresses above the ground [86]. Such biogenic structures allow O₂ transport from the atmosphere to root tips within anoxic sediment, creating a set of oxic micro-niches close to them [11, 53, 56, 58, 75]. Moreover, in French Guiana, these periodically flooded mangroves are known to present significant positive redox potential [63, 64] because of the hydro-sedimentary instability of the surface sediment of mud banks. Thus, aerobic heterotrophic microbial communities could be to a large extent supported and regulated by these phenomena, especially at low tide during the DS, and make the aerobic catabolism the major decomposition pathway, as also described by Alongi et al. [12] in a mangrove with similar TOC characteristics.

In the present study, the MR of mangrove soils was highly variable, a result that is similar to those referenced for other mangrove ecosystems [10, 12, 19, 24, 58, 60] and which is due to heterogeneous micro-environmental characteristics, such as OC content and O₂ availability. The MR values of soils of P facies were the lowest and increased strongly toward soils of older stages, concomitantly with TOC content. Previous studies also reported such respiration patterns across mangrove vegetation profiles [10, 24, 61], indicating that this was likely due to differences in tidal position and flooding duration and subsequent accumulation rates of SOM (e.g., litter). Our results highlighted that if TOC contents are a major structuring factor of MR patterns of soil microbial communities, the TOC quality must also be considered as a determining factor in the expression of microbial metabolism. Moreover, during the two hydroclimatic seasons, similar patterns of MR were observed across the facies. Such stability has been previously reported in other tropical mangroves and interpreted by Alongi [7] and Holmer et al. [48] as a lack of effect of hydroclimatic context on sediment C microbial oxidation. However, during the DS, the MR of NRZ soils of P facies was significantly higher than those of the two RZ soils. As previously suggested, the occurrence of microalgae biofilm on the surface of NRZ mudflat, concomitantly with increased solar irradiation during the DS, may improve both C primary production and oxic conditions, thus explaining the higher MR ratio observed.

Enzyme Activity

The activities of sediment enzymes involved in the main biogeochemical cycles still remain poorly documented in mangrove ecosystems. Thus, another aim of our study was to provide information on enzyme dynamics in such environments.

The activity values obtained were within the range of the few other published studies on enzyme activities of mangrove sediments (Brazil: [16, 27, 38], India: [32, 33], China: [59]). For almost all the enzymes investigated across the

development stages of the Montabo mangrove, the highest values were observed in soils of older stages, which also had the highest TOC contents. Similar observations have also been reported by Dinesh et al. [33] and Liu et al. [59] for other mangrove stands. Moreover, other studies, performed all over the world on non-mangrove sediments, including a large proportion of bare sediments, revealed the same influence of TOC on enzyme activity [22, 26, 55, 87]. Thus, it appears that the TOC is a ubiquitous structuring factor for these microbial functions in soils, including those of mangroves. The strong increase of β -glu activity and even more that of Lip (20- to 50-fold higher) in older stages relative to pioneer stage clearly evidenced an increase in degradation processes of SOM derived from aboveground vegetation. These enzyme activities increased much more than the others in relation with the abundance of their natural substrates, i.e., plant carbohydrates (e.g., cellulose) and lipids (e.g., wax and cutin). This observation indicates an enhancement of aboveground-belowground linkages as succession proceeds, providing a more suitable environment for enzyme synthesis and accumulation in mangrove sedimentary matrix.

Another aim of our work was to investigate, in pioneer stage, the rhizospheric effect of the two mangrove species on enzyme activities. The lack of difference of enzyme activity pattern in this early stage of colonization may indicate a preponderant effect of the SOM mainly derived from marine and micro-phytobenthic input on functional expression of microbial communities.

Functional Diversity

As also mentioned for enzyme patterns, few studies involving CLPPs measurement have been performed on sediments [26, 67], and what is more, only one dealing with the functional diversity of mangrove soil microorganisms [1] has been carried out using Biolog EcoPlates™.

Across the development stages of mangrove, we evidenced a loss of functional diversity and a greater C-source specialization with the increase of TOC content in soils. Within the pioneer stage, no difference between the three kinds of soil was observed, which remained highly diversified in their catabolic profiles. Considering the lower content of the different C pools of the pioneer stage, the increased functional diversities may be *in fine* interpreted as a response of microbial communities toward C starvation, microorganisms being constrained to diversify their C-acquisition mechanisms to survive. Thus, as also suggested for MR, the functional patterns of microbial communities of P facies soils may be much more fuelled and controlled by imported marine OM or by micro-phytobenthos-derived OM [64] than by mangrove vegetation (dead biomass, leachates, and exudates). Moreover, molecular analyses of mobile mud deposits performed by Madrid et al. [62] in French Guiana indicated that bacterial

diversity was among the most diverse of all environments reported to date. Although metagenomic was not investigated in our study, the observations of Madrid et al. [62] may also explain the higher H' 's we found in the pioneer stage; the higher the microbial diversity, the higher are the functions expressed. Considering the F facies, a strong variability of H' was observed for both seasons. This could be explained by the existence of high micro-environmental heterogeneity due to the development of dense and extensive networks of pneumatophores and near-surface roots as well as both the litter inputs and their mineralization products. At local scale, these environmental factors can modify the nutrient availability (e.g., root exudates, litter leachates) and the diversity of catabolic sources, thus resulting in modifications of functional diversity of soil microbial communities [3].

Conclusion

This study has shown that, along a mangrove vegetation profile, physico-chemical characteristics of soils were strongly influenced by both the vegetation cover and the intertidal stands of the different mangrove facies. Among the different pedological parameters, TOC and its different C pools appeared as the main structuring factors for the expression of soil microbial functions. Soil respiration and enzyme activities were enhanced in the more mature mangrove stages, reflecting an increased imprint of aboveground vegetation on these microbial functions. By contrast, in the pioneer stages, the hydro-sedimentary instability, coupled with the poverty of the vegetation cover and the colonization of mud-flat by micro-phytobenthic biofilm, resulted in low C content and low microbial activity. However, in these pioneer facies, the diversity of CLPPs was higher and was interpreted as an improvement of C acquiring potential by microbial communities to counteract C scarcity. From the results of this study, several lines of research would be interesting to develop. Mangrove soils are a mosaic of habitats with very diverse physico-chemical characteristics coexisting at micro-environmental scale. Thus, anaerobic microbial functions, such as anaerobic respiration or anaerobic Biolog CLPP diversity, could be investigated for a better understanding of these complex ecosystems. Concerning Biolog diversity, mesocosm incubations would be also desirable to simulate and understand more precisely the effects of different qualities of C sources on the CLPP patterns of mangrove soils.

Acknowledgments This work has been supported by the Programme Biodiversité Marine of the Direction de l'Environnement, de l'Aménagement et du Logement (DEAL) from French Guiana, and by the Institut de Recherche pour le Développement (IRD) from France. We warmly thank Mrs. Ginette Poitevin and Mr. André Litampha (LAMA, US IRD 191 IMAGO) for their assistance in the laboratory, and Mrs. Annie Guiral and Mr. Thomas Luglia for their help in the field. We also

would like to acknowledge Mr. Michael Paul for improving the English of the manuscript.

References

- Adame MF, Reef R, Herrem-Silveira JA, Lovelock CE (2012) Sensitivity of dissolved organic carbon exchange and sediment bacteria to water quality in mangrove forests. *Hydrobiologia* 691:239–253
- Alarcón-Gutiérrez E, Couchaud B, Augur C, Calvert V, Criquet S (2008) Effects of nitrogen availability on microbial activities, densities and functional diversities involved in the degradation of a Mediterranean evergreen oak litter (*Quercus ilex* L.). *Soil Biol Biochem* 40:1654–1661
- Alarcón-Gutiérrez E, Floch C, Augur C, Le Petit J, Ziarelli F, Criquet S (2009) Spatial variations of chemical composition, microbial functional diversity, and enzyme activities in a Mediterranean litter (*Quercus ilex* L.) profile. *Pedobiologia* 52:387–399
- Alarcón-Gutiérrez E, Floch C, Ruauel F, Criquet S (2008) Non-enzymatic hydrolysis of fluorescein diacetate (FDA) in a Mediterranean oak (*Quercus ilex* L.) litter. *Eur J Soil Sci* 59:139–146
- Allison MA, Lee MT (2004) Sediment exchange between Amazon mudbanks and shore-fringing mangroves in French Guiana. *Mar Geol* 208:169–190
- Alongi DM (1988) Bacterial productivity and microbial biomass in tropical mangrove sediments. *Microb Ecol* 15:59–79
- Alongi DM (1994) The role of bacteria in nutrient recycling in tropical mangrove and other coastal benthic ecosystems. *Hydrobiologia* 285:19–32
- Alongi DM (1996) The dynamics of benthic nutrient pools and fluxes in tropical mangrove forests. *J Mar Res* 54:123–148
- Alongi DM, Christoffersen P, Tirendi F (1993) The influence of forest type on microbial–nutrient relationships in tropical mangrove sediments. *J Exp Mar Biol Ecol* 171:201–223
- Alongi DM, de Carvalho NA, Amaral AL, da Costa A, Trott L, Tirendi F (2012) Uncoupled surface and below-ground soil respiration in mangroves: implications for estimates of dissolved inorganic carbon export. *Biogeochemistry* 109:151–162
- Alongi DM, Tirendi F, Clough BF (2000) Below-ground decomposition of organic matter in forests of the mangroves *Rhizophora stylosa* and *Avicennia marina* along the arid coast of Western Australia. *Aquat Bot* 68:97–122
- Alongi DM, Wattayakorn G, Pfitzner J, Tirendi F, Zagorskis I, Brunskill GJ, Davidson A, Clough BF (2001) Organic carbon accumulation and metabolic pathways in sediments of mangrove forests in southern Thailand. *Mar Geol* 179:85–103
- Anthony EJ, Dolique F, Gardel A, Gratiot N, Proisy C, Polidori L (2008) Nearshore intertidal topography and topographic-forcing mechanisms of an Amazon-derived mud bank in French Guiana. *Cont Shelf Res* 28:813–822
- Baldock JA, Preston CM (1995) Chemistry of carbon decomposition processes in forests as revealed by solid-state carbon-13 nuclear magnetic resonance. In: McFee WW, Kelly JM (eds) Carbon forms and functions in forest soils. Soil Science Society of America, Madison, pp 89–117
- Baltzer F, Allison MA, Fromard F (2004) Material exchange between the continental shelf and mangrove-fringed coasts with special reference to the Amazon–Guianas coast. *Mar Geol* 208:115–126
- Baptista Neto JA, Crapeze MAC, McAlister JJ, Vilela CG (2005) Concentration and bioavailability of heavy metals in sediments from Niterói harbour (Guanabara Bay/S.E. Brazil). *J Coastal Res* 20:1–7
- Bashan Y, Moreno M, Troyo E (2000) Growth promotion of the seawater-irrigated oilseed halophyte *Salicornia bigelovii* inoculated

- with mangrove rhizosphere bacteria and halotolerant *Azospirillum* spp. *Biol Fert Soils* 32:265–272
18. Bétouille JL (1998) Variations spatio-temporelles de la production de litière et des apports en éléments minéraux dans cinq faciès d'une mangrove en Guyane française. Thèse, Université Paul Sabatier, Toulouse III, 168 p
 19. Bouillon S, Borges AV, Castañeda-Moya E, Diele K, Dittmar T, Duke NC, Kristensen E, Lee SY, Marchand C, Middelburg JJ, Rivera-Monroy VH, Smith TJ, Twilley RR (2008) Mangrove production and carbon sinks: a revision of global budget estimates. *Glob Biogeochem Cy* 22:GB2013. doi:10.1029/2007GB003052
 20. Bouillon S, Dahdouh-Guebas F, Rao AVVS, Koedam N, Dehairs F (2003) Sources of organic carbon in mangrove sediments: variability and possible ecological implications. *Hydrobiologia* 495:33–39
 21. Cadamuro L (1999) Structure et Dynamique des écosystèmes inondables (forêt marécageuse, mangrove) du bassin du Sinnamary (Guyane Française). Thèse, Université Paul Sabatier, Toulouse III, 228 p
 22. Caravaca F, Alguacil M, Torres P, Roldán A (2005) Microbial activities and arbuscular mycorrhizal fungi colonization in the rhizosphere of the salt marsh plant *Inula crithmoides* L. along a spatial salinity gradient. *Wetlands* 25:350–355
 23. Chamayou H, Legros JP (1989) Les bases physiques, chimiques et minéralogiques de la science du sol. Agence de Coopération Culturelle et Technique, Paris, 593 p
 24. Chen GC, Tam NFY, Ye Y (2012) Spatial and seasonal variations of atmospheric N₂O and CO₂ fluxes from a subtropical mangrove swamp and their relationships with soil characteristics. *Soil Biol Biochem* 48:175–181
 25. Cook RL, Langford CH, Yamdagni R, Preston CM (1996) A modified cross-polarization magic angle spinning ¹³C NMR procedure for the study of humic materials. *Anal Chem* 68:3979–3986
 26. Costa AL, Paixão SM, Caçador I, Carolino M (2007) CLPP and EEA profiles of microbial communities in salt marsh sediments. *J Soil Sedim* 7:418–425
 27. Crapez MAC, Cavalcante AC, Bispo MGS, Alves PH (2001) Distribuição e atividade enzimática de bactérias nos limites inferior e superior entre-marés na Praia de Boa Viagem, Niterói, R.J., Brasil. In: Moraes R et al (eds) Efeito de poluentes em organismos marinhos. Arte e Ciência, Villipress, São Paulo, pp 129–138
 28. Curtis JT, McIntosh RP (1950) The interrelations of certain analytic and synthetic phytosociological characters. *Ecology* 31:434–455
 29. Dabin B (1967) Application des dosages automatiques à l'analyse des sols. 3^{ème} partie. Méthode Olsen modifiée. *Cah ORSTOM Pedol* 5: 257–286
 30. Debenay JP, Jouanneau JM, Sylvestre S, Weber O, Guiral D (2007) Biological origin of rhythmites in muddy sediments of French Guiana. *J Coastal Res* 23:1431–1442
 31. Dignac MF, Knicker H, Kögel-Knabner I (2002) Effect of N content and soil texture on the decomposition of organic matter in forest soils as revealed by solid-state CP/MAS NMR spectroscopy. *Org Geochem* 33:1715–1726
 32. Dinesh R, Chaudhuri SG, Ganeshamurthy AN, Pramanik SC (2004) Biochemical properties of soils of undisturbed and disturbed mangrove forests of South Andaman (India). *Wetl Ecol Manag* 12:309–320
 33. Dinesh R, Shome BR, Shome R, Bandyopadhyay AK (1998) Soil enzymes in the mangroves: activities and their relation to relevant soil properties. *Curr Sci India* 75:510–512
 34. Eivazi F, Tabatabai MA (1988) Glucosidases and galactosidases in soils. *Soil Biol Biochem* 20:601–606
 35. Fabre A, Fromard F, Trichon V (1999) Fractionation of phosphate in sediments of four representative mangrove stages (French Guiana). *Hydrobiologia* 392:13–19
 36. Fiot J, Gratiot N (2006) Structural effects of tidal exposures on mudflats along the French Guiana coast. *Mar Geol* 228:25–37
 37. Floch C, Capowicz Y, Criquet S (2009) Enzyme activities in apple orchard agroecosystems: how are they affected by management strategy and soil properties? *Soil Biol Biochem* 41:61–68
 38. Fontana LF, Filho JGM, Netto ADP, Santos ESS, de Figueiredo AG Jr, Crapez MAC (2010) Geomicrobiology of cores from Suruí Mangrove–Guanabara Bay–Brazil. *Mar Pollut Bull* 60:1674–1681
 39. Fromard F, Puig H, Mougín E, Marty G, Bétouille JL, Cadamuro L (1988) Structure, above-ground biomass and dynamics of mangrove ecosystems: new data from French Guiana. *Oecologia* 115:39–53
 40. Gardel A, Proisy C, Lesourd S, Philippe S, Caillaud J, Gontharet S, Anthony EJ, Butler L (2009) A better understanding of mud cracking processes gained from in situ measurements on an intertidal mudflat in French Guiana. *J Coastal Res* 56:424–428
 41. Gerbaud G, Ziarelli F, Caldarelli S (2003) Increasing the robustness of heteronuclear decoupling in magic-angle sample spinning solid-state NMR. *Chem Phys Lett* 377:1–5
 42. Grasshoff K, Johannsen H (1972) A new sensitive and direct method for the automatic determination of ammonia in seawater. *ICES J Mar Sci* 34:516–521
 43. Green VS, Stott DE, Diack M (2006) Assay for fluorescein diacetate hydrolytic activity: optimization for soil samples. *Soil Biol Biochem* 38:693–701
 44. Gupta N, Rathi P, Gupta R (2002) Simplified *para*-nitrophenyl palmitate assay for lipases and esterases. *Anal Biochem* 311:98–99
 45. Hatcher PG, Schritzer M, Dennis LW, Maciel GE (1981) Aromaticity of humic substances in soils. *Soil Sci Soc Am J* 45:1089–1094
 46. Hatcher PG, Spiker EC, Szeverenyi NM, Maciel GE (1983) Selective preservation and origin of petroleum-forming aquatic kerogen. *Nature* 305:498–501
 47. Holguin G, Vazquez P, Bashan Y (2001) The role of sediment microorganisms in the productivity, conservation, and rehabilitation of mangrove ecosystems, an overview. *Biol Fert Soils* 33:265–278
 48. Holmer M, Andersen FØ, Holmboe N, Kristensen E, Thong-tham N (1999) Transformation and exchange processes in the Bangrong mangrove forest–seagrass bed system, Thailand. Seasonal and spatial variations in benthic metabolism and sulfur biogeochemistry. *Aquat Microb Ecol* 20:203–212
 49. Hyde KD, Lee SY (1995) Ecology of mangrove fungi and their role in nutrient cycling: what gaps occur in our knowledge? *Hydrobiologia* 295:107–118
 50. Kandeler E, Gerber H (1988) Short-term assay of soil urease activity using colorimetric determination of ammonium. *Biol Fert Soils* 6:68–72
 51. Kathiresan K, Bingham BL (2001) Biology of mangroves and mangrove ecosystems. *Adv Mar Biol* 40:81–251
 52. Kögel-Knabner I (2002) The macromolecular organic composition of plant and microbial residues as inputs to soil organic matter. *Soil Biol Biochem* 34:139–162
 53. Komiyama A, Ong JE, Pongpan S (2008) Allometry, biomass, and productivity of mangrove forests: a review. *Aquat Bot* 89:128–137
 54. Koroleff F (1969) Direct determination of ammonia in natural waters as indophenol blue. *ICES J Mar Sci* 9:19–22
 55. Köster M, Dahlike S, Meyer-Reil LA (1997) Microbiological studies along a gradient of eutrophication in a shallow coastal inlet in the southern Baltic Sea (Nordrügensch Bodden). *Mar Ecol-Prog Ser* 152: 27–39
 56. Kristensen E, Alongi DM (2006) Control by fiddler crabs (*Uca vocans*) and plant roots (*Avicennia marina*) on carbon, iron and sulfur biogeochemistry in mangrove sediment. *Limnol Oceanogr* 51:1557–1571
 57. Kristensen E, Bouillon S, Dittmar T, Marchand C (2008) Organic carbon dynamics in mangrove ecosystems: a review. *Aquat Bot* 89: 201–219
 58. Kristensen E, Mangion P, Tang M, Flindt MR, Holmer M, Ulomi S (2011) Microbial carbon oxidation rates and pathways in sediments of two Tanzanian mangrove forests. *Biogeochemistry* 103:143–158

59. Liu H, Tian Y, Zheng T, Yan C, Hong H (2008) Studies of glucosidase activities from surface sediments in mangrove swamp. *J Exp Mar Biol Ecol* 367:111–117
60. Lovelock CE (2008) Soil respiration and belowground carbon allocation in mangrove forests. *Ecosystems* 11:342–354
61. Lovelock CE, Sorrell BK, Hancock N, Hua Q, Swales A (2010) Mangrove forest and soil development on a rapidly accreting shore in New Zealand. *Ecosystems* 13:437–451
62. Madrid VM, Aller JY, Aller RC, Chistoserdov AY (2001) High prokaryote diversity and analysis of community structure in mobile mud deposits of French Guiana: identification of two new bacterial candidate divisions. *FEMS Microbiol Ecol* 37:197–209
63. Marchand C, Baltzer F, Lallier-Vergès E, Albéric P (2004) Pore-water chemistry in mangrove sediments: relationship with species composition and developmental stages (French Guiana). *Mar Geol* 208: 361–381
64. Marchand C, Lallier-Vergès E, Baltzer F (2003) The composition of sedimentary organic matter in relation to the dynamic features of a mangrove-fringed coast in French Guiana. *Estuar Coast Shelf S* 56: 119–130
65. Massiot D, Fayon F, Capron M, King I, Le Calvé S, Alonso B, Durand JO, Bujoli B, Gan Z, Hoatson G (2002) Modelling one- and two-dimensional solid-state NMR spectra. *Magn Reson Chem* 40:70–76
66. Mathers NJ, Mendham DS, O'Connell AM, Grove TS, Xu Z, Saffigna PG (2003) How does residue management impact soil organic matter composition and quality under *Eucalyptus globulus* plantations in southwestern Australia? *Forest Ecol Manag* 179:253–267
67. Min K, Kang H, Lee D (2011) Effects of ammonium and nitrate additions on carbon mineralization in wetland soils. *Soil Biol Biochem* 43:2461–2469
68. Olsen SR, Cole CV, Watanabe FS, Dean LA (1954) Estimation of available phosphorus in soils by extraction with sodium bicarbonate. USDA Circular 939:1–19
69. Peersen OB, Wu X, Kustanovich I, Smith SO (1993) Variable-amplitude cross-polarization MAS NMR. *J Magn Reson* 104: 334–339
70. Peltier A (1993). Caractérisation et dynamique des mangroves de Guyane française. Rapport de stage de DEA, ENS-Paris VI, 39 p + annexes
71. Pesarin F (2001) Multivariate permutation tests with applications in biostatistics. Wiley, Chichester, 408 p
72. Pongpam S, Komiyama A, Tanaka A, Sangtuan T, Makruak C, Kato S, Tanapempool P, Patanaponpaiboon P (2009) Carbon dioxide emission through soil respiration in a secondary mangrove forest of eastern Thailand. *J Trop Ecol* 25:393–400
73. Preston CM, Schnitzer M, Ripmeester JA (1989) A spectroscopic and chemical investigation on the de-astringing of a humin. *Soil Sci Soc Am J* 53:1142–1147
74. Preston CM, Trofymow JA, Sayer BG, Niu JN (1997) C-13 nuclear magnetic resonance spectroscopy with cross-polarization and magic-angle spinning investigation of the proximate-analysis fractions used to assess litter quality in decomposition studies. *Can J Botany* 75: 1601–1613
75. Purnobasuki H, Suzuki M (2005) Aerenchyma tissue development and gas-pathway structure in root of *Avicennia marina* (Forsk.) Vierh. *J Plant Res* 118:285–294
76. Quideau SA, Anderson MA, Graham RC, Chadwick OA, Trumbore SE (2000) Soil organic matter processes: characterization by ¹³C NMR and ¹⁴C measurements. *Forest Ecol Manag* 138:19–27
77. Rodier J, Geoffroy C, Kovacsik G, Laporte J, Plissier M, Scheidhauer J, Verneaux J, Vial J (1978) L'analyse de l'eau - Eaux naturelles, eaux résiduaires, eau de mer, 6ème édition. Bordas, Paris, 1136 p
78. Schaefer J, Stejskal EOR (1976) Carbon-13 nuclear magnetic resonance of polymers spinning at magic angle. *J Am Chem Soc* 98: 1031–1032
79. Schmidt MWL, Knicker H, Hatcher PG, Kögel-Knabner I (1997) Improvement of ¹³C and ¹⁵N CPMAS NMR spectra of bulk soils, particle size fractions and organic material by treatment with 10% hydrofluoric acid. *Eur J Soil Sci* 48:319–328
80. Sjöling S, Mohammed SM, Lyimo TJ, Kyaruzi JJ (2005) Benthic bacterial diversity and nutrient processes in mangroves: impact of deforestation. *Estuar Coast Shelf S* 63:397–406
81. Skjemstad JO, Clarke P, Taylor JA, Oades JM, Newman RH (1994) The removal of magnetic materials from surface soils. A solid state ¹³C CPMAS N.M.R. study. *Aust J Soil Res* 32:1215–1229
82. Sylvestre F, Guiral D, Debenay JP (2004) Modern diatom distribution in mangrove swamps from the Kaw Estuary (French Guiana). *Mar Geol* 208:281–293
83. Tabatabai MA (1994) Soil Enzymes. In: Weaver RW, Angle S, Bottomley P, Bezdicek D, Smith S, Tabatabai A, Wollum A (eds) Methods of soil analysis, part 2. Microbiological and biochemical properties. Soil Science Society of America, Madison, pp 775–834
84. Tabatabai MA, Bremner JM (1969) Use of *p*-nitrophenyl phosphate for assay of soil phosphatase activity. *Soil Biol Biochem* 1:301–307
85. Tabatabai MA, Bremner JM (1970) Arylsulphatase activity of soils. *Soil Sci Soc Am Pro* 34:225–229
86. Thonlinson PB (1986) The botany of mangrove. Cambridge University Press, Cambridge, 406 p
87. Wobus A, Bleul C, Maassen S, Sheerer C, Schuppler M, Jacobs E, Röske I (2003) Microbial diversity and functional characterization of sediments from reservoirs of different trophic state. *FEMS Microbiol Ecol* 46:331–347